Highlights of Spanish Astrophysics XI, Proceedings of the XV Scientific Meeting of the Spanish Astronomical Society held on September 4–9, 2022, in La Laguna, Spain. M. Manteiga, L. Bellot, P. Benavidez, A. de Lorenzo-Cáceres, M. A. Fuente, M. J. Martínez, M. Vázquez- Acosta, C. Dafonte (eds.), 2023

The interplay of internal and external processes in the buildup of disk galaxies: thick disks in AURIGA simulations.

Pinna, F.[1], Walo-Martín, D.[2,3], and Grand, R. J. J.[2,3]

[1] Max Planck Institute for Astronomy, Koenigstuhl 17, D-69117 Heidelberg, Germanyemail: pinna@mpia.de
[2]Instituto de Astrofísica de Canarias, Calle Vía Láctea s/n, E-38205 La Laguna, Tenerife, Spain
[3]Departamento de Astrofísica, Universidad de La Laguna, Av. del Astrofísico Francisco Sánchez s/n, E-38206, La Laguna, Tenerife, Spain

Abstract

Recent integral-field spectroscopy observations have revealed that thick- and thin-disk star-formation histories are regulated by the interplay of internal and external processes. We analyze stellar-population properties of 24 spiral galaxies from the AURIGA zoom-in cosmological simulations, to offer a more in-depth interpretation of observable properties. We extracted edge-on maps of stellar age, metallicity and [Mg/Fe] abundance, and star-formation and chemical-evolution histories of thin and thick disks. These show signs of the interplay between internal chemical enrichment and gas and star accretion. Thick disks show particularly complex stellar populations, including an in-situ component, formed from both enriched and more pristine accreted gas, and a significant fraction of ex-situ stars.

1 Introduction

The spatially resolved stellar-population analysis of massive galactic disks allows us to draw the spatial and temporal distribution of star formation during the mass assembly of disk-dominated galaxies. Properties of thick disks, old, metal poor and enhanced in α elements, trace mostly the early stages of galaxy formation, while younger metal-rich thin disks tell us about later evolutionary phases [7, 14]. While it is clear that thin disks form mostly in situ with their massive star formation being fuelled by gas accretion, there is no common agreement on how thick disks form. Three main formation scenarios were proposed to explain thick-disk properties: their stars may have formed in situ, at high redshift, from turbulent gas [2], in satellites that were later directly accreted [1], or in a preexisting thinner disk which was later dynamically heated [3].

Observational studies of thick disks are generally based on edge-on galaxies, where fainter thick disks can be morphologically decomposed from the bright thin disks [5]. Spectroscopic studies have revealed some variety in thick-disk properties, pointing towards one or another formation scenario [6, 9, 14]. On the other hand, detailed star-formation and chemical-evolution histories of thick disks, extracted from deep integral-field spectroscopic MUSE observations, have recently unveiled a combination of in-situ and ex-situ stellar populations. Thick disks would result from complex scenarios with different mechanisms at play [10, 11, 12]. Here we probe these combined scenarios using numerical simulations.

2 Simulations, sample selection and data analysis

The AURIGA project [8] includes zoom-in magneto-hydrodynamical cosmological simulations of 30 Milky Way-mass late-type galaxies, with stellar masses between 10^{10} and $\sim 10^{11}\,\mathrm{M}_\odot$. These were obtained by re-simulating 30 relatively isolated haloes from the parent largest-volume Dark Matter Only EAGLE simulation [13]. The galaxy formation model, including star formation, stellar and black-hole feedback and magnetic fields, led to realistic galaxies matching a large variety of properties found in observed galaxies (e.g. morphologies and properties of structures such as spiral arms or bars, galaxy sizes and masses, kinematic and chemical properties). The initial conditions to be used in the re-simulations, and in particular the initial distribution of dark-matter particles, were taken from the haloes in the parent simulation. Then, each dark-matter particle was substituted by a pair of a dark-matter particle and a gas cell. AURIGA simulations offer different resolution levels [8], and we use "level 4" in this work, corresponding to typical masses of high-resolution dark-matter and baryonic-mass particles of $\sim 3 \times 10^5\,\mathrm{M}_\odot$ and $\sim 5 \times 10^4\,\mathrm{M}_\odot$, respectively. The physical gravitational softening length for stellar and high-resolution dark-matter particles was set to 369 pc at redshift $z < 1$.

From the original sample of 30 galaxies, we selected a sample of 24 with a clear disk structure and no strong distortions due to mergers. We projected the galaxies in an edge-on view, to allow a similar analysis to what is usually done in integral-field spectroscopy observations. We performed a Voronoi binning to ensure a similar number of star particles in each spatial bin and we used for the analysis a region of radius the optical radius R_{opt} of the galaxy [8] and of height $2 \times h_{scale}$, where h_{scale} is the standard deviation of the vertical positions of stars at R_{opt}. For each galaxy, we fitted vertical luminosity-density profiles, extracted in four radial bins, with two components associated with the thin and the thick disks, each one represented by a hyperbolic secant square function. The fits gave us the average height, for each galaxy, at which the light of the thick disk starts to dominate. This allows us to define the thick and the thin disks in a purely geometrical way, using the same definition that is usually adopted in edge-on external galaxies [4, 6, 10, 11, 12]. We show in Fig. 1 mock images, of a size of 50 kpc×20 kpc, of the 24 galaxies in our sample. We indicate with orange dashed horizontal lines the height above (below) which the thick disk starts to dominate. The region between these lines is dominated by the thin disk. For one galaxy, Au1, we obtained a good fit only when using one disk component instead of two, indicating that this galaxy does not have a clear double-disk structure.

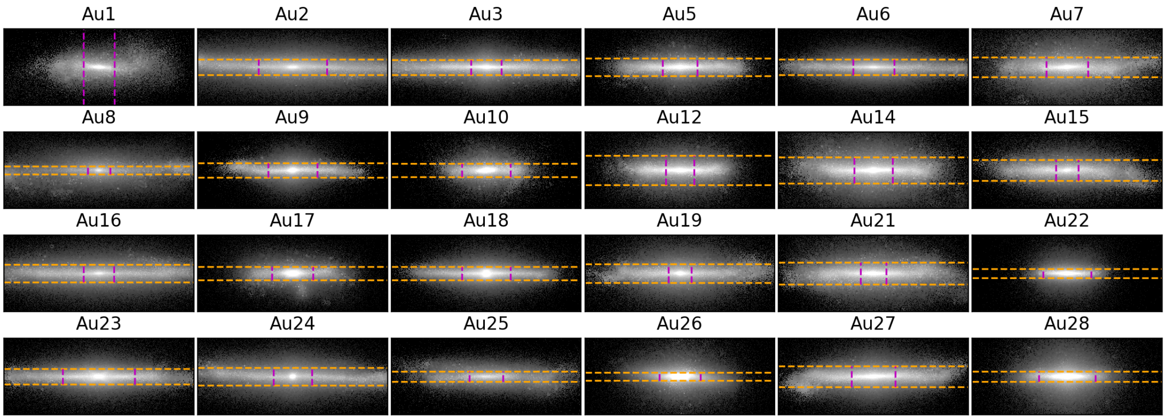

Figure 1: Mock V-band edge-on images of our selected sample of 24 Milky Way-like galaxies from AURIGA simulations. The region showed here has a 50 kpc×20 kpc size. The two orange dashed horizontal lines indicate where the light of the thin-disk component dominates over the thick disk (between the two lines), and where the thick disk dominates (above and below that region). The region between the two vertical magenta dashed lines is dominated by a central component (a bar in barred galaxies and a classical bulge in non-barred galaxies).

3 Results and discussion

Stellar populations. We mapped the stellar populations of the 24 galaxies. In the thick-disk regions, we found a variety of ages, with average values respectively between 5 and 9 Gyr. Average total metallicities ([M/H]) are between -0.2 and 0.1 dex, and [Mg/Fe] abundances between 0.12 and 0.17. A sharp change in the stellar-population parameters corresponds to the transition between the thick- and thin-disk dominated regions (Pinna et al., in prep.). In Fig. 2, we summarize and compare the stellar-population properties of thick and thin disks. Each point indicates the average age, [M/H] or [Mg/Fe] (respectively in the left, middle and right panels) calculated in the thick- and the thin-disk dominated regions. Thick disks are in all cases older, more metal-poor and more [Mg/Fe] enhanced than thin disks. We have color coded each point according to the total stellar mass of the galaxy. While a general trend of the thick- and thin-disk properties with galaxy stellar mass is not clear, galaxies with the lowest masses show smaller differences between the properties of the thin and the thick disks (points closer to the one-to-one line).

We extracted the star-formation histories of the thin and thick disks, in terms of the mass fraction of stars of a specific age, averaging the age distribution in the regions dominated by each one of them [10, 11, 12]. We color coded age bins according to their average metallicity and [Mg/Fe] abundance, to interpret these plots in terms of chemical evolution. Star-formation histories of the full sample can be found in Pinna et al. (in prep.), while we describe an example later in this section.

In-situ and ex-situ components. To assess the ex-situ formation scenario of thick disks, we tracked star particles during the simulations, and classified them as in situ or ex situ. We

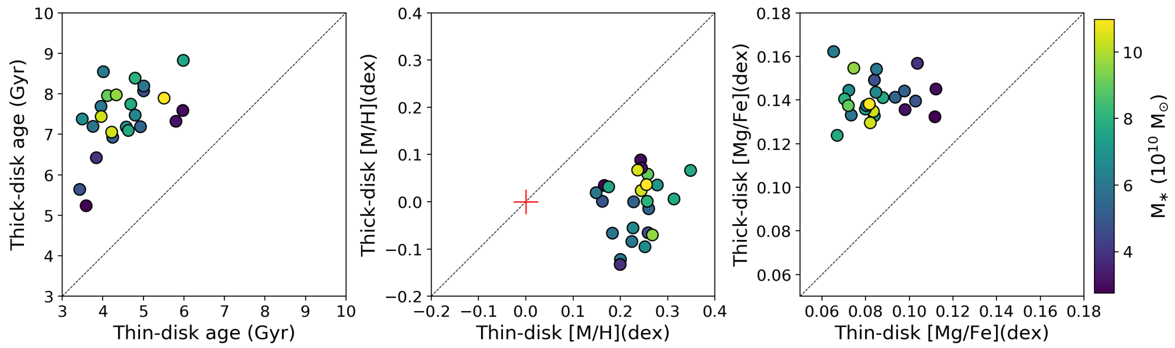

Figure 2: Thick-disk versus thin-disk stellar-population properties. From left to right: age, [M/H] and [Mg/Fe] abundance. Points are color coded according to the total stellar mass of the galaxy. The one-to-one line is indicated as black dashed, in each panel. A red "+" symbol indicates solar metallicity in the middle panel.

mapped the fraction of accreted stars for the full galaxy sample, and found that they are mostly located in the thick-disk dominated region (see Pinna et al., in prep.). Thick disks host a fraction of accreted stars between 5 and 65% of their mass, depending on the specific galaxy. The accreted mass is less than 50% in most cases, and thick disks are therefore mostly formed in situ with a strong contribution from satellites.

A representative galaxy: Au5. We show here one specific galaxy as an example, Au5, representative of our sample. Au5 is a barred spiral galaxy of stellar mass $\sim 7 \times 10^{10} M_{\odot}$. Stellar-population maps of Au5 are shown in Fig. 3, and show an old, metal-poor and [Mg/Fe]-enhanced thick disk and a young, very metal-rich and poorly [Mg/Fe]-enhanced thin disk. We show in Fig. 4 (left panels) the star-formation history of the thick disk in Au5, color coded by [M/H] (top panels) and [Mg/Fe] (bottom panels). At the oldest ages (until about 12 Gyr ago), we see a global increase in the star-formation rate (or the mass fraction in each age bin, evolving across time from right to left in each panel), and a later decrease at young ages (from about 7 Gyr ago to now), with numerous star-formation bursts across the galaxy life. The colors display a global chemical enrichment, transitioning from metal-poor values and a strong [Mg/Fe] enhancement at the oldest ages, to slightly subsolar metallicities and slightly supersolar [Mg/Fe] values at very recent times. However, on top of this global trend, both [M/H] and [Mg/Fe] respectively drop or rise back to previous values, on different occasions across the thick-disk evolution. Similar features are found in most galaxies of our sample.

In order to understand the origin of these [M/H] and [Mg/Fe] oscillations, which often correspond to star-formation bursts, we decomposed the star-formation histories into in-situ and ex-situ components, and revealed that the oscillations in the chemical abundances are driven by the combination of these two components. In Au5 (Fig. 4, middle and right panels), a satellite contributed ~35% of the thick-disk mass. This satellite had its own chemical evolution (right panels), and an enhanced chemical enrichment during the star-formation burst at the final stage of the merger (at ages of about 7 Gyr; note that these higher metallicities are still much lower than the thin-disk values). The in-situ component

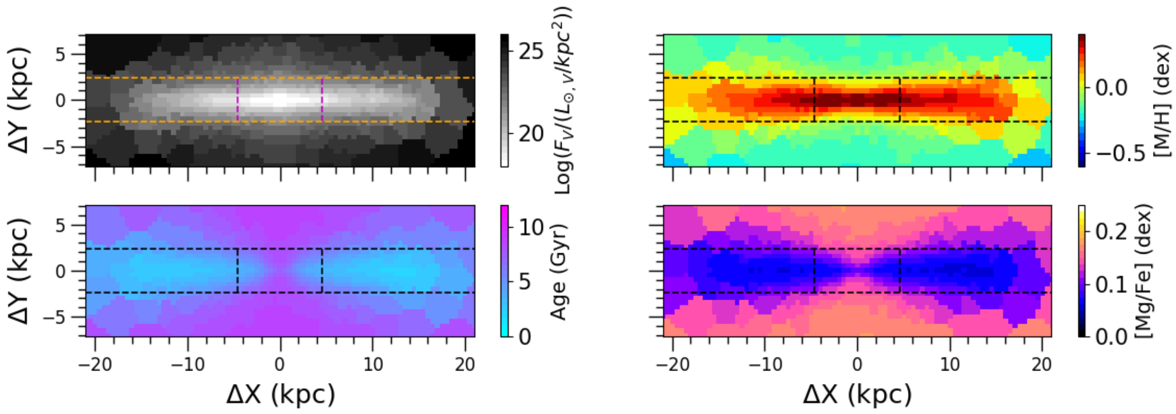

Figure 3: Maps of the galaxy Au5 covering a central region of size $2R_{opt} \times 4h_{scale}$. Logarithmic luminosity density (top-left panel), age (bottom-left panel), [M/H] (top-right panel), and [Mg/Fe] abundance (bottom-right panel). Dashed horizontal lines indicate the distance from the midplane at which the thick disk starts to dominate. The region between the dashed vertical lines is dominated by the bar.

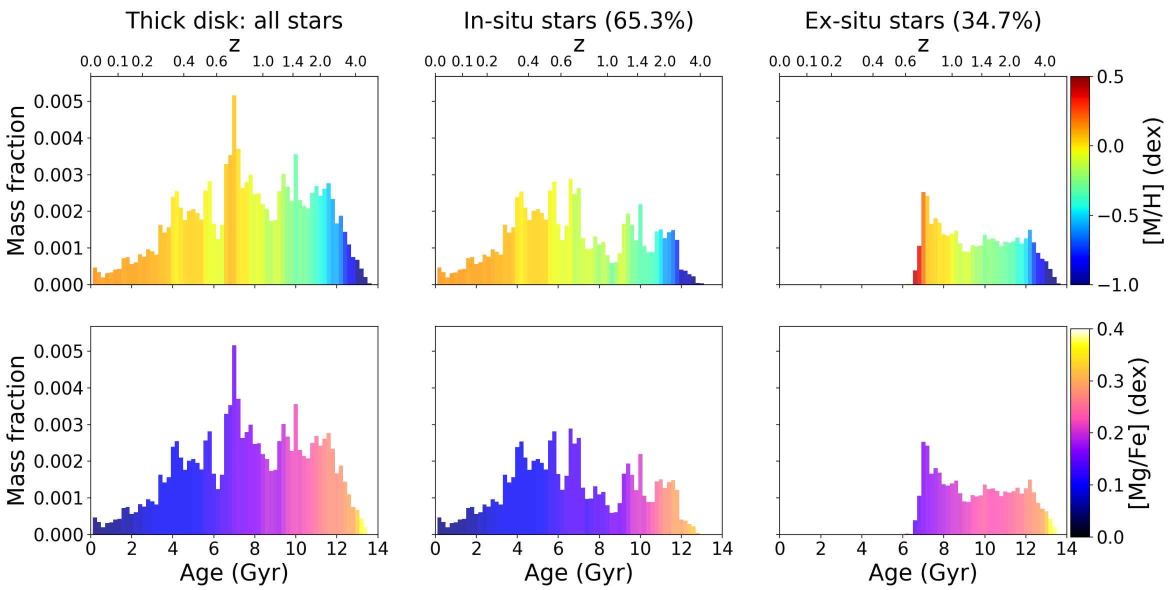

Figure 4: Star-formation history of the thick disk in Au5, color-coded by [M/H] (top panels) and [Mg/Fe] abundance (bottom panels). Left panels include all stars, while middle and right panels include only stars formed respectively in situ or ex situ. The corresponding mass fraction (over the total thick-disk mass) is indicated on top of each column.

(middle panels) is characterized by several star-formation bursts with lower metallicity values (and higher [Mg/Fe]) than immediately younger and older ages. These drops in metallicity are driven by the accretion of gas, mostly coming from the satellite.

4 Conclusions

We analyze the properties of thick and thin disks in a sample of 24 spiral galaxies from AURIGA simulations. Thick and thin disks were defined geometrically in an edge-on projection, according to the regions where their light dominates. Similarly to what was previously found in most observations [4, 7, 9, 10, 12], thick disks are older, more metal poor and [Mg/Fe] enhanced than thin disks. We investigated the fraction of in-situ and ex-situ particles and their contribution in the star-formation histories of thick disks. These results show that although most of the thick-disk mass was formed in situ, but with an important contribution of gas accreted at the time of frequent mergers, they host a significant fraction of accreted stars (in some cases, even most of their mass). Thin disks, as expected from previous observations [7, 10], host a very low mass fraction of accreted stars, and the bulk of their mass was formed at recent times thanks to a large amount of accreted gas.

Star-formation histories of thick and thin disks, and thus of disk galaxies, result from the interplay of internal and external processes: the internal chemical enrichment is challenged by the accretion of more pristine gas and more metal-poor stars.

References

[1] Abadi, M. G., Navarro, J. F., Steinmetz, M., et al., 2003, ApJ, 597, 21.

[2] Brook, C. B., Kawata, D., Gibson, B. K., et al., 2004, ApJ, 612, 894.

[3] Di Matteo, P., Lehnert, M. D., Qu, Y., et al., 2011, A&A, 525, L3.

[4] Comerón, S., Salo, H., Janz, J., et al. 2015, A&A, 584, A34.

[5] Comerón, S., Salo, H., Knapen, J. H. 2018, A&A, 610, A5.

[6] Comerón, S., Salo, H., Knapen, J. H., et al., 2019, A&A, 623, A89.

[7] Gallart, C., Bernard, E. J., Brook, C. B., et al. 2019, Nature Astronomy, 3, 932.

[8] Grand, R. J. J., Gómez, F. A., Marinacci, F., et al. 2017, MNRAS, 467, 179.

[9] Kasparova, A. V., Katkov, I. Y., Chilingarian, I. V., et al. 2016, MNRAS, 460, L89.

[10] Martig, M., Pinna, F., Falcón-Barroso, J., et al. 2021, MNRAS, 508, 2458.

[11] Pinna, F., Falcón-Barroso, J., Martig, M., et al. 2019, A&A, 623, A19.

[12] Pinna, F., Falcón-Barroso, J., Martig, M., et al. 2019, A&A, 625, A95.

[13] Schaye, J., Crain, R. A., Bower, R. G., et al. 2015, MNRAS, 446, 521

[14] Yoachim, P., & Dalcanton, J. J. 2008, ApJ, 683, 707.